Journal of the Endocrine Society, 2023, **7**, 1–16
https://doi.org/10.1210/jendso/bvad034
Advance access publication 28 February 2023
Research Article

Mitoguardin2 Is Associated With Hyperandrogenism and Regulates Steroidogenesis in Human Ovarian Granulosa Cells

Ming-Qi Yan,[1,2,*] Yong Wang,[3,*] Zhao Wang,[4] Xiao-Hong Liu,[5] Yu-Meng Yang,[1] Xiu-Yun Duan,[1] Hui Sun,[3] and Xiao-Man Liu[1,3]

[1]Central Laboratory, Shandong Provincial Hospital Affiliated to Shandong First Medical University, Shandong Provincial Hospital, Shandong University, Jinan 250021, China
[2]School of Life Sciences, Faculty of Science, The Chinese University of Hong Kong, Shatin, N.T., China
[3]Department of Clinical Laboratory Medicine, Shandong Provincial Hospital Affiliated to Shandong First Medical University, Institute of Clinical Microbiology, Shandong Academy of Clinical Medicine, Jinan 250021, China
[4]Center for Reproductive Medicine, Shandong University, Key Laboratory for Reproductive Endocrinology of Ministry of Education, Jinan 250012, China
[5]Department of Infection Control, Jen Ching Memorial Hospital, Kunshan 215300, China

Correspondence: Xiao-Man Liu, PhD, Central Laboratory, Shandong Provincial Hospital Affiliated to Shandong First Medical University, Shandong Provincial Hospital, Shandong University, 544 Jingsi Rd, Jinan, China 250021. Email: liuxiaoman@sdfmu.edu.cn.
*These authors contributed equally to this work.

Abstract

Polycystic ovary syndrome (PCOS) is an endocrinopathy characterized by hyperandrogenism, anovulation, and polycystic ovaries, in which hyperandrogenism manifests by excess androgen and other steroid hormone abnormalities. Mitochondrial fusion is essential in steroidogenesis, while the role of mitochondrial fusion in granulosa cells of hyperandrogenic PCOS patients remains unclear. In this study, mRNA expression of mitochondrial fusion genes mitoguardin1, −2 (*MIGA 1, −2*) was significantly increased in granulosa cells of hyperandrogenic PCOS but not PCOS with normal androgen levels, their mRNA expression positively correlated with testosterone levels. Dihydrotestosterone (DHT) treatment in mice led to high expression of MIGA2 in granulosa cells of ovulating follicles. Testosterone or forskolin/ phorbol 12-myristate 13-acetate treatments increased expression of MIGA2 and the steroidogenic acute regulatory protein (StAR) in KGN cells. MIGA2 interacted with StAR and induced StAR localization on mitochondria. Furthermore, MIGA2 overexpression significantly increased cAMP-activated protein kinase A (PKA) and phosphorylation of AMP-activated protein kinase (pAMPK) at T172 but inhibited StAR protein expression. However, MIGA2 overexpression increased *CYP11A1*, *HSD3B2,* and *CYP19A1* mRNA expression. As a result, MIGA2 overexpression decreased progesterone but increased estradiol synthesis. Besides the androgen receptor, testosterone or DHT might also regulate MIGA2 and pAMPK (T172) through LH/choriogonadotropin receptor-mediated PKA signaling. Taken together, these findings indicate that testosterone regulates MIGA2 via PKA/AMP-activated protein kinase signaling in ovarian granulosa cells. It is suggested mitochondrial fusion in ovarian granulosa cells is associated with hyperandrogenism and potentially leads to abnormal steroidogenesis in PCOS.

Key Words: mitochondrial fusion, testosterone, granulosa cells, steroidogenic acute regulatory protein, sex hormones, polycystic ovary syndrome

Abbreviations: AMPK, AMP-activated protein kinase; AR, androgen receptor; BMI, body mass index; CYP11A1, cytochrome P450 family 11 subfamily A member 1; CYP19A1, cytochrome P450 family 19 subfamily A member 1; DHT, dihydrotestosterone; DRP1, dynamin-related protein 1; E2, estradiol; ER, endoplasmic reticulum; ERMCS, ER-mitochondrial membrane contact site; Flu, flutamide; FSK, forskolin; HA-PCOS, 75 hyperandrogenic PCOS; hCG, human chorionic gonadotropin; HSD3B2, 3 beta-hydroxysteroid dehydrogenase-isomerase 2; IMM, inner mitochondrial membrane; LET, letrozole; LHCGR, LH/choriogonadotropin receptor; MFN1, mitofusin 1; MFN2, mitofusin 2; MIGA1, mitoguardin 1; MIGA2, mitoguardin 2; mtDNA, mitochondrial DNA; NA-PCOS, 54 normo-androgenic PCOS; OMM, outer mitochondrial membrane; OPA1, optic atrophy 1; pAMPK, phosphorylation of AMPK; PCOS, polycystic ovary syndrome; PKA, cAMP-activated protein kinase A; PLD6, mitochondrial phospholipase mito PLD; PMA, phorbol 12-myristate 13-acetate; PMSG, pregnant mare serum gonadotropin; PRKACA, PKA catalytic subunit α; PRKACB, PKA catalytic subunit β; qRT-PCR, quantitative RT-PCR; StAR, steroidogenic acute regulatory protein; T, testosterone; TOMM20, translocase of outer mitochondrial membrane 20.

Polycystic ovary syndrome (PCOS) is a complex endocrine and metabolic disorder, commonly characterized by hyperandrogenism, ovulation dysfunction, and polycystic ovary morphologic features. PCOS affects about 6% to 10% of reproductive-aged women according to different diagnostic criteria [1, 2]. PCOS women are generally accompanied by hyperandrogenism, hyperinsulinemia, LH hypersecretion, and disordered intrafollicular endocrine, which leads to the accumulation of small antral follicles [3]. Approximately 60% to 80% of PCOS patients present with hyperandrogenism [4], and more than 60% of PCOS patients have functional ovarian hyperandrogenism [5]. Recent studies revealed that the 11-oxygenated 19-carbon steroids produced primarily from the adrenal cortex

Received: 30 November 2022. **Editorial Decision:** 23 February 2023. **Corrected and Typeset:** 15 March 2023

substantially contribute to hyperandrogenemia in women with PCOS [6]. Hyperandrogenemia was proved to successfully induce hyperinsulinemia and insulin resistance in a PCOS mouse model [7].

Recent findings indicated that mitochondrial dysfunction [ie, oxidative stress, altered mitochondrial DNA (mtDNA) copy number, and altered mitochondrial dynamics] was associated with PCOS [8-10]. Oxidative stress impaired mitochondrial function and had been found to be increased in women with PCOS [11]. Alterations in mtDNA copy number and mutations in mtDNA were widely found in the peripheral blood of PCOS patients [12, 13]. Mitochondrial dynamics regulates mitochondrial mass and morphology, leading to changes in mitochondrial function (ie, mitochondrial respiration activity, reactive oxygen species and mtDNA stability) [14, 15]. Recent studies indicated that the mitochondrial fission dynamin-related protein 1 (DRP1) was increased in granulosa cells of a dihydrotestosterone (DHT)-induced PCOS model in rat [16]. Gene expression of some key steroidogenic enzymes localized to mitochondria, such as cytochrome P450 family 11 subfamily A member 1 (CYP11A1) and steroidogenic acute regulatory (StAR), was altered in granulosa cells from the small antral follicles of PCOS women [17]. These findings suggest that mitochondrial dysfunctions mediated by the disordered mitochondrial dynamics may be associated with hyperandrogenism and contribute to the abnormal steroidogenesis in PCOS, while the role of mitochondrial fusion in steroidogenesis in ovarian granulosa cells of PCOS women with hyperandrogenism warrants further investigation.

Mitochondria play a crucial role in steroidogenesis, a process involving a series of rate-limiting enzymes localized on the mitochondrial membrane. Steroidogenesis is initiated by the translocation of cholesterol from the cytosol to mitochondria. To transport the cholesterol to the inner mitochondrial membrane (IMM), cholesterol is first delivered and inserted into the outer mitochondrial membrane (OMM) through transduceosome. The main components of the transduceosomal machinery include StAR, translocator protein, voltage-dependent anion-selective channel, acetyl-coenzyme binding domain-containing 3 and ATPase family AAA domain-containing protein 3 [18, 19]. The translocase of outer mitochondrial membrane 20 (TOMM20) is an initial docking site for proteins with mitochondrial presequences. StAR is synthesized as a pre-protein with an N-terminal mitochondrial presequence (37 KDa) and is cleaved to yield an intramitochondrial mature protein (30 KDa); it fuses to the C-terminus of TOMM20 and exerts its activity exclusively on the OMM [20]. StAR contains 2 conserved sites for phosphorylation by the protein kinase A (PKA) and the phosphorylation was key for the steroidogenic activity of StAR [21]. LH induces the elevation of cAMP through LH/choriogonadotropin receptor (LHCGR) and activates PKA, then StAR is rapidly activated and transfers cholesterol to the IMM, thus making the cholesterol available to the CYP11A1 enzyme system. CYP11A1 catalyzes the conversion of cholesterol to pregnenolone, and the pregnenolone is mainly converted by 3 beta-hydroxysteroid dehydrogenase (HSD3B) to progesterone. HSD3B is mainly encoded by 2 genes: *HSDB1* and *HSDB2*. *HSDB1* is exclusively expressed in placenta and peripheral tissues such as skin ,while the HSDB2 gene is predominantly expressed in steroidogenic tissues of adrenals, testis, and the ovary [22]. The cytochrome P450 family 19 subfamily A member 1 (CYP19A1; aromatase) catalyzes aromatization of androgens to synthesize estrogens [23, 24].

Recently it was found granulosa cells of PCOS patients showed dysfunctions of mitochondria and defects in glucose metabolism [25]. Testosterone was found to activate glucose metabolism through AMPK signaling in cardiomyocyte hypertrophy, a high risk for offspring of PCOS patients [26]. AMPK is a cellular energy sensor that is activated by the phosphorylation of AMPK at Thr172 (T172) and is key for mitochondrial homeostasis [27]. However, AMPK and LH/PKA were found to regulate steroidogenesis in an opposite way in luteal cells [28]. PKA catalytic subunits are mainly coded by PRKACA and PRKACB genes, which exhibit different gene expression patterns and functions [29]. However, whether and how testosterone or DHT regulates mitochondrial fusion through AMPK or PKA signaling remains unknown.

In previous studies, the mitochondrial proteins of mitoguardin 1 (MIGA1) and mitoguardin 2 (MIGA2) were found to mediate the OMM fusion through the mitochondrial phospholipase MitoPLD (PLD6) [30]. Except for mitochondrial fusion, MIGA2 exerted more functions through the links with endoplasmic reticulum (ER)-mitochondrial membrane contact site (ERMCS) and lipid droplet in adipocytes [31, 32]. The structural basis of MIGA2 for ERMCS formation and lipid trafficking has been revealed recently [33]. By knocking out *Miga1* or *Miga2* in mice, the progesterone levels were significantly reduced in serum or in ovarian granulosa cells, leading to ovulation disruption and female subfertility [34]. In the current study, mitochondrial fusion was proposed to be disturbed in ovarian granulosa cells of PCOS women with hyperandrogenism. Expression of *MIGA1, −2* was detected in granulosa cells of PCOS patients with hyperandrogenism and the controls; their expression levels were analyzed with the serum testosterone levels. To study the mechanism of MIGA1, −2 functions in PCOS with hyperandrogenism, we applied KGN cell line, which is a steroidogenic human ovarian granulosa-like tumor cell line, widely acknowledged as a valuable model for studying steroidogenesis [35]. The present study aims to reveal that high levels of androgen might regulate mitochondrial fusion mediated by MIGA1, −2 which might regulate steroidogenesis through PKA/AMPK signaling in ovarian granulosa cells.

Materials and Methods

Sample Collections

This study was approved by the Ethics Committee of Center for Reproductive Medicine, Shandong University for experiments with humans. Informed consents were obtained from female subjects ages 21 to 35 years old. Granulosa cells were collected from 129 PCOS women [75 hyperandrogenic PCOS (HA-PCOS), 54 normo-androgenic PCOS (NA-PCOS)] and 82 controls. The controls consisted of women who had normal endocrine and performed in vitro fertilization-embryo transfer or intracytoplasmic sperm injection. Diagnosis of PCOS was confirmed according to the Rotterdam Criteria [36], which required at least 2 of the following 3 characteristics: chronic oligo- or anovulation, clinical or biochemical manifestations of hyperandrogenism, polycystic ovary morphology. Patients with other etiologies of hyperandrogenemia such as Cushing's syndrome, androgen-secreting tumors, nonclassical congenital adrenal hyperplasia, and oral contraceptive use were excluded.

Wildtype mice (C57/BL6) (obtained from Beijing Vital River Laboratory Animal Technology Co., Ltd.) were housed in a 12:12 hours light and dark schedule. Female mice at postnatal day 21 to 23 were injected with 5 international units (IU) pregnant mare serum gonadotropin (PMSG) (Ningbo Sansheng Pharmaceutical Co., China) for 44 hours and 5 IU human chorionic gonadotropin (hCG) (Ningbo Sansheng Pharmaceutical Co., China) as control or 5 IU hCG plus 100 μg DHT for 8 hours/16 hours [37]. All animals were handled with care according to the Animal Research Committee guidelines of Shandong Provincial Hospital Affiliated to Shandong First Medical University.

Steroid Measurement

Serum samples were collected on the second to the fifth day of the menstrual cycle for women with regular menstruation or randomly for women with irregular menstruation. Cell medium samples were harvested in 12-well plate. Concentrations of total testosterone (T), dehydroepiandrosterone sulfate, estradiol (E2), and progesterone were measured by chemiluminescence (Roche Diagnostics, Germany). The laboratory measuring the hormones was certified by the National Center for Clinical Laboratories, and the correlation coefficients of variation for intra-assay and inter-assay precision were less than 10%, which were lower than the limits of acceptability (15%).

Cell Culture

Human mural granulosa cells were isolated by density gradient centrifugation from the follicular fluid of the patients who received oocyte retrieval after stimulation with hCG for 36 hours. Mouse granulosa cells were harvested from the ovary 24 hours after injection of PMSG [38]. KGN cells (obtained from RIKEN BioResource Center, Ibaraki, Japan) were cultured in DMEM/F-12 medium (HyClone, UT, USA), supplemented with 10% fetal bovine serum (HyClone, UT, USA) and antibiotics (100 IU/mL penicillin, 100 μg/mL streptomycin) (Sigma, Saint Louis, USA). Cells were cultured at 37 °C in a humidified environment with 5% CO2. Forskolin (FSK; 10 mM) and phorbol 12-myristate 13-acetate (PMA; 20 nM) (Sigma) were used to induce luteinization of the granulosa cells *in vitro* for 24 hours. Testosterone (Sigma) at different doses were used to detect the responses of the granulosa cells.

Lentivirus Production and Infection

The cDNA sequences of human mitoguardin 1 (*MIGA1*) and mitoguardin 2 (*MIGA2*) were both attached with FLAG-tag sequence (DYKDDDDK). Lentivirus vectors were prepared using the psPAX2, pMD2.G and PHBLV^{TM} expression systems. Replication-defective recombinant lentiviruses were grown, propagated, and tittered on HEK293T cells. Then they were used to infect KGN cells in multiple assays. GFP-expressing lentivirus was used as a control during infection. Transfection efficiency was confirmed by detecting the expression of mRNAs or proteins of target genes through quantitative RT-PCR (qRT-PCR) and western blotting.

Immunoprecipitation Assay and Western Blotting

For the immunoprecipitation assay, total proteins were lysed from the cells and centrifuged at 12 000 rpm for 15 minutes; the supernatant was incubated with FLAG, MIGA2, or StAR antibody at 4°C overnight and then incubated with Protein A/G magnetic beads (Millipore, Billerica, USA) for 4 hours at 4°C. The beads were washed 3 times with PBST (0.1% Tween) buffer, and SDS loading buffer was added for western blotting assay. For western blotting assay, each sample was loaded with 10 to 15 μg of protein. They were separated through the SDS-PAGE) and transferred to polyvinylidene difluoride membranes. After being blocked in 5% skim milk, the membranes were incubated with primary antibodies at 4°C overnight. Information of the antibodies used in this study is listed in Table 1. The polyvinylidene difluoride membranes were incubated in horseradish peroxidase-conjugated secondary antibodies (Thermo Fisher Scientific catalog no. 31460, RRID:AB_228341; 31430, RRID:AB_228307) and specifically in light chain specific secondary antibody for endogenous MIGA2 in the immunoprecipitation assay. Then the membranes were detected with chemiluminescent HRP Substrates (Millipore, Billerica, MA, USA). Finally, the bands were observed and photographed with GelDoc2 XR Gel Documentation System (BioRad, Hercules, CA, USA), and analyzed with the Image J software.

qRT-PCR

Total RNA was extracted with TRIzol Reagent (Invitrogen, Carlsbad, CA, USA) and was templated for their cDNA by reverse transcription using Prime Script RT reagent Kit with gDNA Eraser (TaKaRa, Japan). The qRT-PCR was performed using the SYBR® Green PCR Master Mix (TaKaRa, Japan) and analyzed on the LightCycler 480 II Real-Time PCR instrument (Roche, Germany). Relative mRNA expression of genes was calculated using the comparative crossing points method with GAPDH as the reference gene and the formula $2^{-\triangle\triangle Cp}$ [39]. Relative quantification of the mRNA was presented as fold change according to the control. The detailed information of primers has been listed in Supplementary Table S1 [40].

Immunofluorescence

Cells were fixed in 4% paraformaldehyde for 30 minutes, permeated with 0.1% Triton X-100 for 10 minutes, blocked with 5% BSA for 30 minutes, and incubated with primary antibodies at 4°C overnight. After washing, the cells were incubated with secondary antibodies conjugated with fluorescent dyes in dark for 30 minutes at room temperature. Cells were mounted on slides in VECTASHIELD Mounting Medium with DAPI antibody (Vector Laboratories catalog no. H-1200, RRID: AB_2336790) and imaged by the confocal microscope of Leica TCS SP8 microsystem (Leica, Germany). Information on the relevant antibodies is listed in Table 1.

Immunohistochemistry

Ovaries were fixed in 4% paraformaldehyde and embedded in paraffin. The sections were stained with immunohistochemistry using the method as reported [34]. Ovary sections were incubated with primary antibody, reacted with biotin-labeled secondary antibodies (Vector Laboratories catalog no. PK-6100, RRID:AB_2336819), and stained with a 3, 3V-diaminobenzidine peroxidase substrate kit (Vector Laboratories catalog no. SK-4100, RRID:AB_2336382). Sections were counterstained with hematoxylin and analyzed with the TissueFAXS Plus system (Tissue Gnostics, Austria). Information on the relevant primary antibody is listed in Table 1.

Table 1. Information of antibodies used in this study

Antibodies	RRID	Source company	Catalog number	Working concentration	Description
Anti-MIGA2 (FAM73B)	AB_11129174	Abcam	ab122713	WB: 1:1000; IHC: 1:200; IP: 1:100	Rabbit polyclonal
Anti-MIGA1 (FAM73A)	AB_11129122	Abcam	ab121532	WB: 1:1000	Rabbit polyclonal
Anti-FLAG	AB_10950495	Cell Signaling Technology	8146	WB: 1:1000; IP:1:50	Mouse monoclonal
Anti-LHCGR	AB_2135467	Santa Cruz	sc-25828	WB: 1:50	Mouse monoclonal
Anti-StAR	AB_10889737	Cell Signaling Technology	8449	WB: 1:1000; IP: 1:50; IF: 1:100	Rabbit monoclonal
Anti-TOMM20	AB_945896	Abcam	ab56783	IF: 1:2000; WB: 1:5000	Mouse monoclonal
Anti-MFN2	AB_2266320	ProteinTech	12186-1-AP	WB: 1:1000	Rabbit polyclonal
Anti-OPA1	AB_944549	Abcam	ab42364	WB: 1:1000	Rabbit polyclonal
Anti-PRKACA	AB_2766136	ProteinTech	27398-1-AP	WB: 1:1000	Rabbit polyclonal
Anti-PRKACB	AB_10949078	ProteinTech	55382-1-AP	WB: 1:1000	Rabbit polyclonal
Anti-AMPK α	AB_330331	Cell Signaling Technology	2532	WB: 1:1000	Rabbit polyclonal
Anti-phospho-AMPK α (T172)	AB_331250	Cell Signaling Technology	2535	WB: 1:1000	Rabbit monoclonal
Anti-β-Tubulin	AB_2881629	ProteinTech	66240-1-Ig	WB: 1:5000	Mouse monoclonal
Anti-β-ACTIN	AB_2223172	Cell Signaling Technology	4970	WB: 1:1000	Rabbit monoclonal
Anti-GAPDH	AB_2107436	ProteinTech	#60004-1-Ig	WB: 1:1000	Mouse monoclonal
HRP conjucted Rabbit IgG (light chain Specific)	AB_2800208	Cell Signaling Technology	#93702S	WB:1:2000	Mouse monoclonal

Statistical Analysis

Data are presented as the mean ± standard deviation. Statistical comparisons were made using one-way ANOVA and Tukey's test for multiple comparisons. Student's t-test was used for comparisons between 2 groups for normally distributed variables and the Kolmogorov-Smirnov test for nonparametric test. Pearson or Spearman's correlation coefficient was analyzed to estimate the interrelationships (GraphpadPrism8, California, USA). All experiments were repeated at least 3 times; the coefficients of variation for intra-assay were less than 10%, and inter-assay was less than 15% for all the data generated from the cultured cells. Differences with $P < .05$ were considered statistically significant.

Results

MIGA1, –2 Expression is Associated With Testosterone Levels in Human Granulosa Cells

Baseline characteristics of the control, HA-PCOS, and NA-PCOS subjects are described in Supplementary Table S2 [40]. Subjects of HA-PCOS exhibited higher body mass index (BMI), serum testosterone, and E2 levels than control and the NA-PCOS. To examine the correlation of testosterone and gene expression of *MIGA1*, –2, the mRNA levels of *MIGA1* and *MIGA2* were detected in granulosa cells of the subjects. It was found that mRNA levels of *MIGA1* and *MIGA2* both increased significantly in the HA-PCOS subjects compared with the controls or NA-PCOS subjects (Fig. 1A and 1B). As a result, the serum testosterone levels were positively correlated with both *MIGA1* ($P < .01$) and *MIGA2* ($P < .01$) mRNA levels in all the subjects (Fig. 1C and 1D). Additional findings showed that serum testosterone positively correlated with BMI (Fig. 1E), and the expression of MIGA2 but not MIGA1 was also positively correlated with BMI in human granulosa cells (Fig. 1F and 1G), suggesting that the expression of MIGA2 in granulosa cells might play a role in body lipid formation in PCOS females. These data indicated that the expression of *MIGA1* and *MIGA2* genes in human granulosa cells was associated with serum testosterone levels. Accordingly, expression of MIGA1 and MIGA2, especially MIGA2, was supposed to be associated with abnormal steroidogenesis and lipid formation in ovarian granulosa cells of PCOS.

MIGA2 Regulates Progesterone and Estradiol Levels in Human Granulosa Cells

To assess the steroidogenic functions of MIGA1, –2 in human ovarian granulosa cells, MIGA1 and MIGA2 overexpression

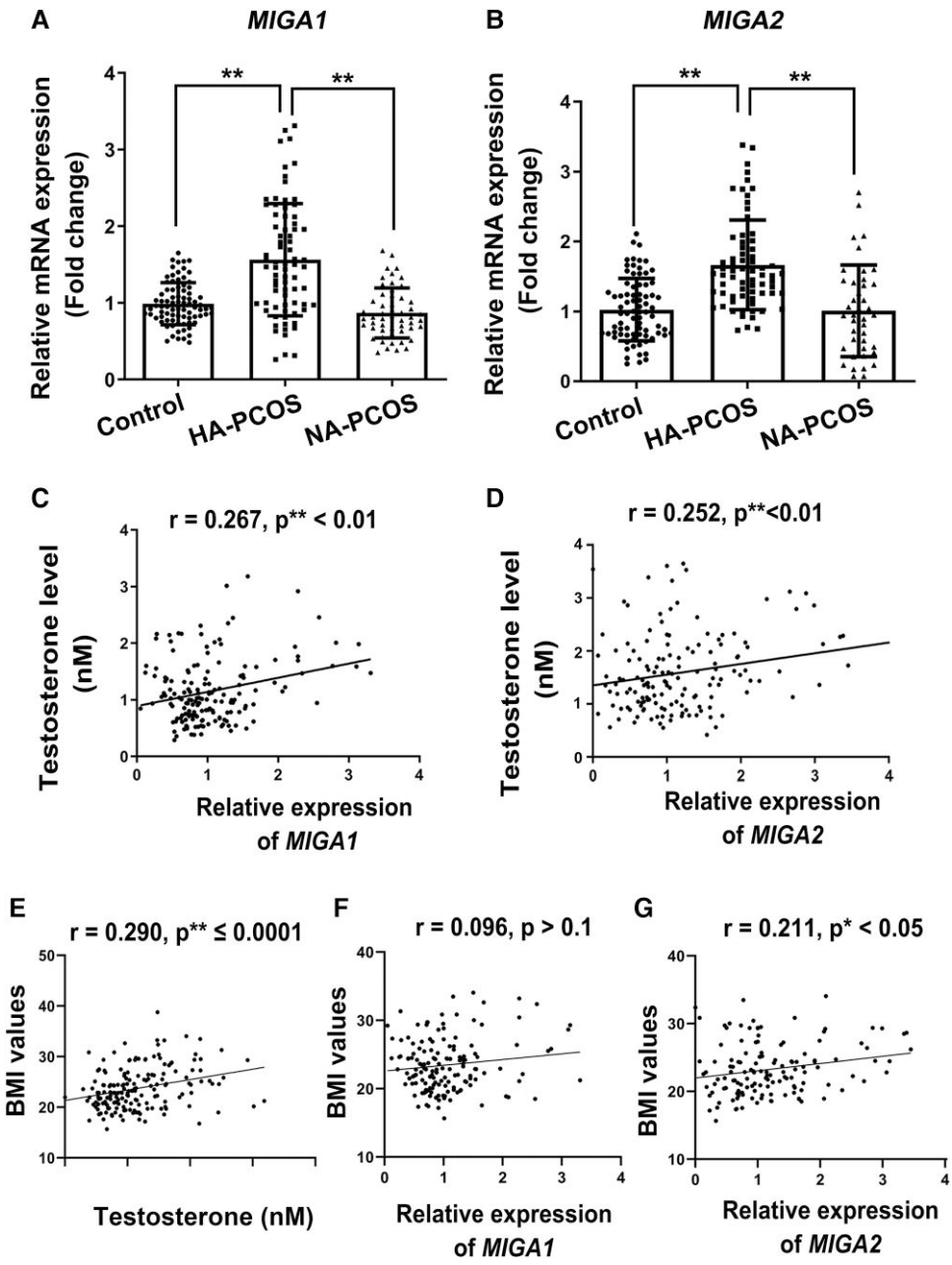

Figure 1. MIGA1 and MIGA2 expression levels are increased in granulosa cells of hyperandrogenic PCOS and correlates with serum testosterone in human. (A, B) Relative mRNA expression of *MIGA1* and *MIGA2* in patients of the control, HA-PCOS, and NA-PCOS groups. (C, D) Correlation of the relative expression of *MIGA1*(C) and *MIGA2* (D) to testosterone in all the subjects. (E-G) Correlation of the BMI values with serum testosterone levels (E) and the relative expression of *MIGA1* (F) and *MIGA2* (G) in granulosa cells. Data presented as mean ± SD. **, $P < .01$. The Spearman rank correlation was used to calculate *r* and *P*-values according to the distribution of relevant variables.
Abbreviations: BMI, body mass index; HA-PCOS, 75 hyperandrogenic PCOS; MIGA1, mitoguardin 1; MIGA2, mitoguardin 2; NA-PCOS, 54 normoandrogenic PCOS; PCOS, polycystic ovary syndrome.

lentiviruses were transfected in KGN cells. Protein levels of MIGA1 and MIGA2 were positively detected after lentivirus transfection; FSK/PMA treatment for 24 hours significantly increased MIGA1 and MIGA2 expression compared with the nontreatment controls (Fig. 2A). Overexpression of GFP-tagged MIGA1 or MIGA2 altered mitochondria morphology to an aggregated state after 24 hours of FSK/PMA treatment (Fig. 2B). Interestingly, MIGA2 overexpression significantly increased the mRNA expression of *CYP11A1*, *CYP19A1*, and *HSD3B2* genes after FSK/PMA treatment for 24 hours (Fig. 2C). As a result, MIGA2 overexpression significantly reduced progesterone levels (Fig. 2D) while slightly increased E2 levels after FSK/PMA treatment for 24 hours (Fig. 2E). Testosterone addition resulted in an overall increase in progesterone levels, without significant difference between the control and MIGA1, −2 overexpression (Fig. 2F). However, MIGA2 overexpression significantly increased the E2 levels after adding testosterone (Fig. 2G), indicating that MIGA2 overexpression could significantly promote the conversion of testosterone to E2 in human granulosa cells. To assess whether MIGA2 expression was associated with E2 synthesis, the aromatase (CYP19A1) inhibitor

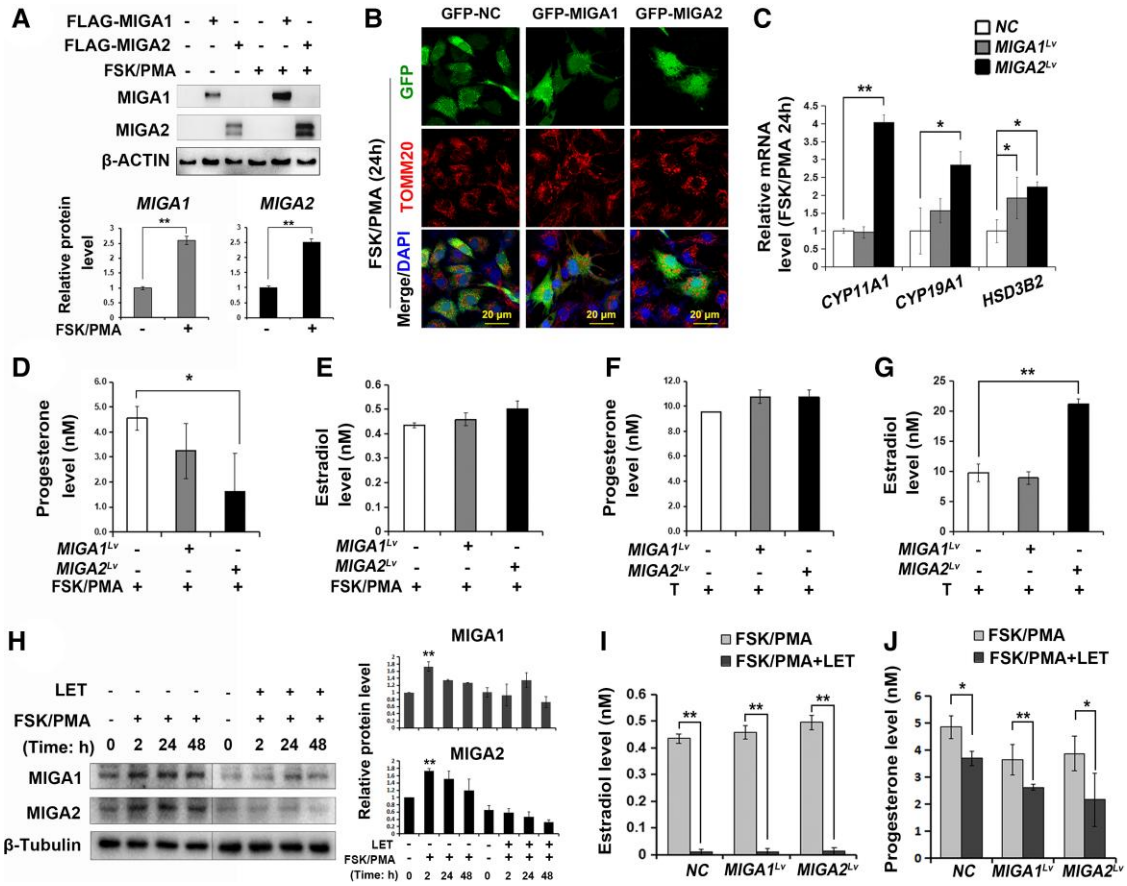

Figure 2. MIGA2 regulates progesterone and estradiol by regulating steroidogenesis-related genes in KGN cells. (A) Representative western blots of MIGA1 and MIGA2 after transfection of *MIGA1* or *MIGA2* overexpression lentiviruses and treatments with FSK/PMA for 24 hours or not and the quantification of relative MIGA1 and MIGA2 protein levels after FSK/PMA treatment to untreated samples. (B) Confocal images of immunofluorescence of TOMM20 in GFP-tagged MIGA1 and MIGA2 overexpressing cells after FSK/PMA treatment for 24 hours. (C) Relative expression of the steroidogenesis related genes of *CYP11A1*, *CYP19A1*, *HSD3B2* after *MIGA1, −2* overexpression, and treatments with FSK/PMA for 24 hours. (D, E) Progesterone (D) and estradiol (E) hormone levels after *MIGA1* or *MIGA2* overexpression and treatments of FSK/PMA for 24 hours. (F, G) Progesterone (F) and estradiol (G) hormone levels after transfection of *MIGA1* or *MIGA2* overexpression lentiviruses and treatments of testosterone (100 nM) for 24 hours. (H) Representative western blot of MIGA1 and MIGA2 after FSK/PMA or combined with LET treatments for the indicated times, and the quantitative analysis of relative expression of MIGA1 and MIGA2 proteins after the above treatments. (I) Estradiol levels after *MIGA1* or *MIGA2* overexpression and treatments with FSK/PMA or combined with LET for 24 hours. (J) Progesterone levels after *MIGA1* or *MIGA2* overexpression and treatments with FSK/PMA or combined with LET for 24 hours. Data presented as mean ± SD. *, $P < .05$, **, $P < .01$.
Abbreviations: FSK, forskolin; LET, letrozole; MIGA1, mitoguardin 1; MIGA2, mitoguardin 2; PMA, phorbol 12-myristate 13-acetate; TOMM20, translocase of outer mitochondrial membrane 20.

letrozole (LET) was used in combination with FSK/PMA compounds. MIGA1 and MIGA2 protein expression was induced after FSK/PMA treatment for different times as indicated, while LET addition suppressed the FSK/PMA-induced MIGA1 and MIGA2 expression (Fig. 2H), suggesting that CYP19A1 activity might be essential for FSK/PMA-induced MIGA1, −2 expression. Consequently, the E2 levels were greatly suppressed by LET in all cells with or without MIGA1, −2 overexpression, and progesterone levels were decreased after combined treatment of LET with FSK/PMA compared with FSK/PMA treatment alone (Fig. 2I and 2J). Briefly, overexpression of MIGA2 regulated steroidogenesis in luteinized human granulosa cells resulting in low progesterone levels and high E2 levels.

MIGA1, −2 Regulate Expression of Mitochondrial Fusion Proteins and StAR

Overexpression efficiency of *MIGA1* and *MIGA2* in KGN cells was positively detected. The mRNA levels of *MIGA1, −2* were significantly increased after lentivirus transfection. Interestingly, MIGA1 overexpression could significantly increase the expression of other mitochondrial fusion genes of *MIGA2*, *MFN2*, *OPA1*, and *PLD6*, while MIGA2 overexpression only promoted significant expression of *MFN2* and *OPA1* (Fig. 3A and 3B), which suggested a different role of MIGA1 and MIGA2 in granulosa cells. After FSK/PMA or testosterone treatment for 24 hours, expression of MIGA1 and MIGA2 protein levels was detected by the FLAG tag (Fig. 3C). It was found that MIGA1 or MIGA2 overexpression increased MFN2, OPA1, and TOMM20 protein levels after FSK/PMA treatment for 24 hours; testosterone addition further increased their protein levels compared with the FSK/PMA treatment alone, while MIGA2overexpression suppressed the increase of MFN2, OPA1, and TOMM20; especially TOMM20 expression was significantly reduced compared with the controls treated with FSK/PMA and testosterone for 24 hours (Fig. 3C and 3D). However, MIGA2 overexpression significantly reduced StAR protein levels after treatment with FSK/PMA for 24 hours, and testosterone

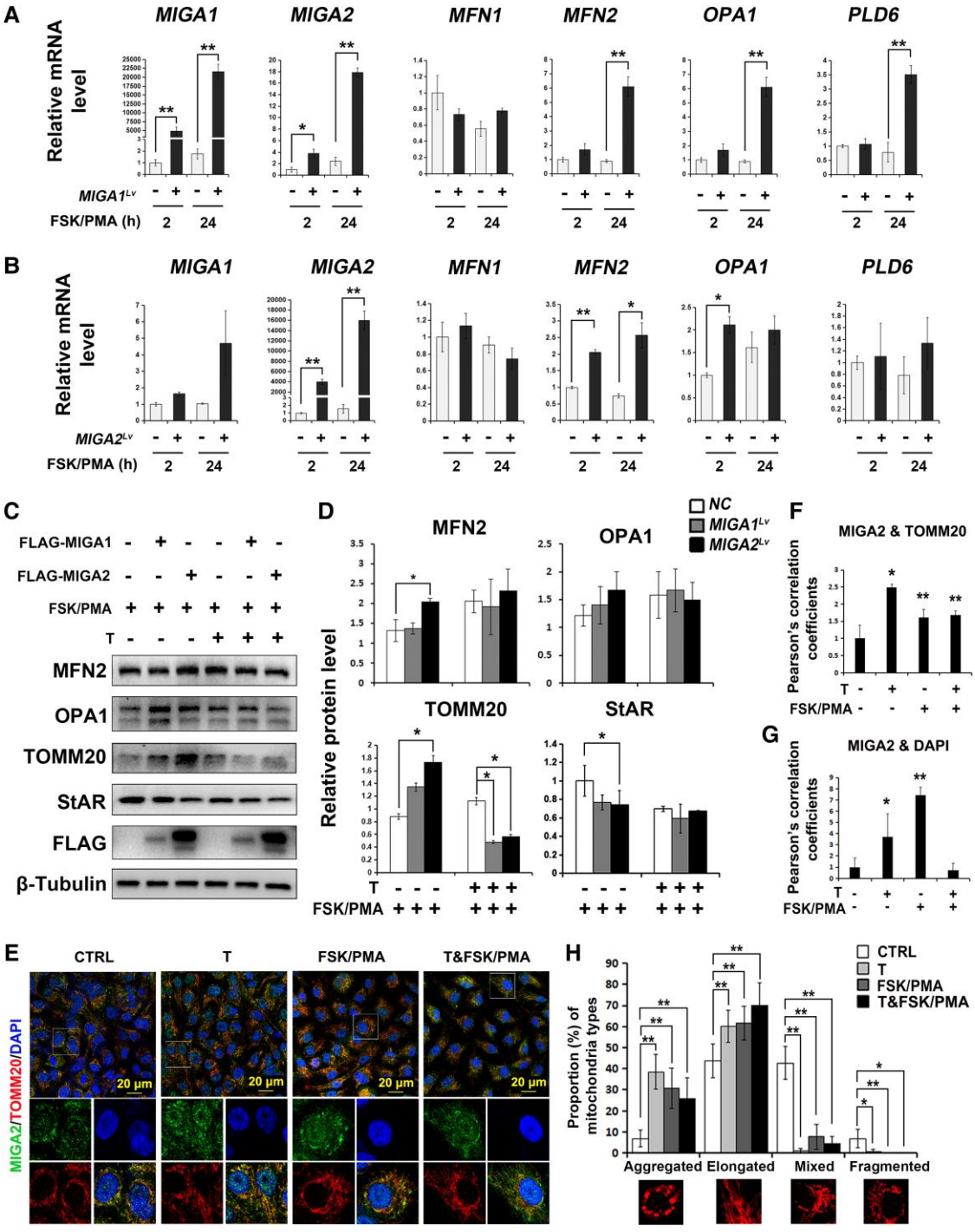

Figure 3. MIGA1, –2 regulate mitochondrial fusion protein and StAR expression and are regulated by testosterone and FSK/PMA in KGN cells. (A, B) Relative mRNA expression of mitochondrial dynamic genes of *MIGA1, –2, MFN1, –2, OPA1,* and *PLD6* after overexpression of MIGA1 (A) or MIGA2 (B) with FSK/PMA treatment for 2 or 24 hours. (C, D) Representative western blots images (C) and their quantification (D) of MFN2, OPA1, TOMM20, StAR, and FLAG after *MIGA1* or *MIGA2* overexpression with FSK/PMA or testosterone treatments for 24 hours. (E) Confocal microscopy images for immunofluorescence of MIGA2 and TOMM20 counterstained with the nucleus dye DAPI in cells treated with testosterone or FSK/PMA for 24 hours. (F, G) Pearson's correlation coefficients of MIGA2 and TOMM20 (F), MIGA2, and DAPI (G) were analyzed from the data of (E). Their statistical significance of difference was compared to the control. (H) Statistical analysis of different types of mitochondrial morphology was carried out from the data of E. The mitochondrial morphology was divided into 4 types: aggregated, elongated, mixed, and fragmented types. Data presented as mean ± SD. *, $P < .05$, **, $P < .01$.
Abbreviations: FSK, forskolin; MIGA1, mitoguardin 1; MIGA2, mitoguardin 2; OPA1, optic atrophy 1; PMA, phorbol 12-myristate 13-acetate; StAR, steroidogenic acute regulatory protein; TOMM20, translocase of outer mitochondrial membrane 20.

addition decreased StAR expression further when compared with the controls (Fig. 3C and 3D). To detect the endogenous MIGA2 expression, confocal microscopy images were captured after testosterone or FSK/PMA treatments in KGN cells. They showed testosterone, FSK/PMA, or their combined treatments increased the colocalization of MIGA2 and TOMM20 (Fig. 3E and 3F). In addition, testosterone or FSK/PMA treatments increased the nucleus localization of

MIGA2, while the increase in nucleus localization was abolished after the combined treatments of testosterone and FSK/PMA (Fig. 3E and 3G). Also, the majority of mitochondrial morphology was shown to be aggregated or elongated after testosterone, FSK/PMA, or their combined treatments (Fig. 3H).

Testosterone or DHT Regulates MIGA2 and StAR Expression in Ovarian Granulosa Cells

Testosterone or DHT was used to detect the actions of high levels of androgen on MIGA2 and StAR expression in KGN cells. It was shown that testosterone significantly increased MIGA2 protein expression, while the effect of DHT on increasing MIGA2 protein expression was compromised (Fig. 4A and 4B). In contrast, both testosterone and DHT significantly increased StAR protein expression levels, while the effect of testosterone on increasing StAR protein expression was stronger than that of DHT (Fig. 4A and 4C). In addition, FSK/PMA treatment significantly increased MIGA2 and StAR protein expression in a time-dependent manner; MIGA2 showed a significant increase with FSK/PMA treatment for 4 to 6 hours, while StAR showed a significant increase with FSK/PMA treatment for 4 to 24 hours (Fig. 4D-F). However, progesterone levels were significantly decreased after adding testosterone (10-200 nM) with FSK/PMA treatment for 24 hours (Fig. 4G). It was found testosterone (10-1000 nM) significantly reduced the expression of MIGA2 protein after the combined treatment of FSK/PMA for 24 hours, but DHT did not show significant differences (Fig. 4H and 4I); meanwhile, testosterone (100-1000 nM) or DHT (100-1000 nM) both significantly reduced StAR protein expression (Fig. 4H and 4J). This suggested that the reduced expression levels of MIGA2 and StAR might contribute to the decrease of progesterone levels.

In addition, the mRNA expression of *LHCGR* was increased with testosterone (100 nM) or FSK/PMA treatment compared with control, and the other important steroidogenic genes of *CYP11A1*, *CYP19A1,* and *HSD3B2* were all increased after testosterone treatment (Fig. 4K). Furthermore, it was found testosterone, FSK/PMA, or their combined treatment could significantly induce StAR expression and its localization on mitochondria (Fig. 4L-N). DHT treatment in vivo elevated Miga2 expression in mouse granulosa cells treated with PMSG 48 hours/hCG 8 hours or 16 hours, especially in ovulating follicles that were treated with PMSG 48 hours/hCG 16 hours compared with controls, while Miga2 expression was further decreased in luteal cells compared to granulosa cells in the ovulating follicles (Fig. 4O). To examine the expression of the steroidogenic genes in mouse granulosa cells, we isolated the mouse primary granulosa cells and treated the cells with testosterone and FSK/PMA in vitro. The results showed that the *Cyp19a1* expression was increased by FSK/PMA treatment for 2 hours but decreased after the combined treatment of testosterone and FSK/PMA for 2 hours, while the expression of the sulfotransferase family 1E, member 1, which was important for E2 metabolic, was reduced by testosterone treatment but further increased by FSK/PMA or combined treatment with testosterone (Supplementary Fig. S1A) [40]. *Lhcgr* expression was increased by the treatment of testosterone or FSK/PMA for 24 hours, whereas their combined treatment significantly increased the expression. While *StAR* mRNA expression was increased by FSK/PMA treatment but decreased by the combined treatment of testosterone and FSK/PMA, and *Cyp11a1* and *Hsd3b1* expression were both increased by FSK/PMA or the combined treatment of testosterone and FSK/PMA for 24 hours (Supplementary Fig. S1B) [40].

In addition, Miga2 expression in mouse theca cells seemed to be increased in DHT-treated mouse ovaries with PMSG 48 hours/hCG 8 hours or 16 hours. To test whether Miga2 actioned in theca cells, mouse theca cells were isolated from the ovaries and transfected with the MIGA1 and MIGA2 overexpression lentivirus to detect testosterone levels. As a result, overexpression of MIGA1 or MIGA2 led to an increase in testosterone levels in theca cells (Fig. 4P), which might be the manner of serum testosterone function on the follicular cells.

To identify whether E2, a byproduct of testosterone, directly regulated MIGA2 expression or mitochondrial morphology, E2 was used to treat cells. The results showed that proportion of aggregated mitochondria was significantly increased after E2 (1-10 nM) treatment for 24 hours, and the other mitochondria types were relatively decreased compared with the control cells (Fig. 4Q and 4R). In addition, E2 (1-100 nM) could also increase MIGA2 protein expression but not StAR protein in a concentration-dependent manner; however, treatment of E2 at 10-100 nM combined with FSK/PMA for 24 hours decreased expression of MIGA2 and StAR proteins (Fig. 4S).

These results suggested that testosterone could partially mimic LH functions and regulate the expression of MIGA2 in human granulosa cells. Testosterone exerted a stronger function than that of DHT, which might be attributed to the action of E2.

MIGA1, –2 Form Complexes With StAR in Human Granulosa Cells

To verify whether MIGA1 and MIGA2 interact with StAR in human granulosa cells, FLAG-tagged human MIGA1 and MIGA2 lentiviruses were transfected and treated with FSK/PMA for 24 hours in KGN cells. As a result, FLAG-tagged human MIGA1 and MIGA2 were found to interact and form complexes with StAR, and overexpression of MIGA1 or MIGA2 could enhance the interaction with StAR on mitochondria (Fig. 5A). To detect endogenous interaction between MIGA2 and StAR, the cells were treated with testosterone (100 nM), DHT (100 nM), or FSK/PMA for 24 hours. After immunoprecipitation with MIGA2, interactions of MIGA2 and StAR were detected after testosterone or DHT treatments; after immunoprecipitation with StAR, the interaction of MIGA2 and StAR was also detected after testosterone or FSK/PMA treatment. However, when the cells were treated with DHT, the recognition epitopes of StAR protein might be masked by the interacting protein complexes; StAR failed to be pulled down and the interaction with MIGA2 was undetectable (Fig. 5B). This further confirmed that MIGA2 and StAR interacted with each other endogenously. Furthermore, MIGA1 and MIGA2 were found to increase StAR localization on mitochondria after FSK/PMA treatment for 24 hours compared to controls, with increases in the Pearson's correlation coefficients between StAR and TOMM20 and between MIGA1, 2-GFP and StAR (Fig. 5C-E). These data suggested that MIGA1/2 might suppress StAR protein expression but induce StAR localization on mitochondria through protein interactions.

Testosterone Regulates MIGA2 Expression Partially Through the Androgen Receptor

To identify whether testosterone regulates MIGA1, –2 through the androgen receptor (AR), we used the AR

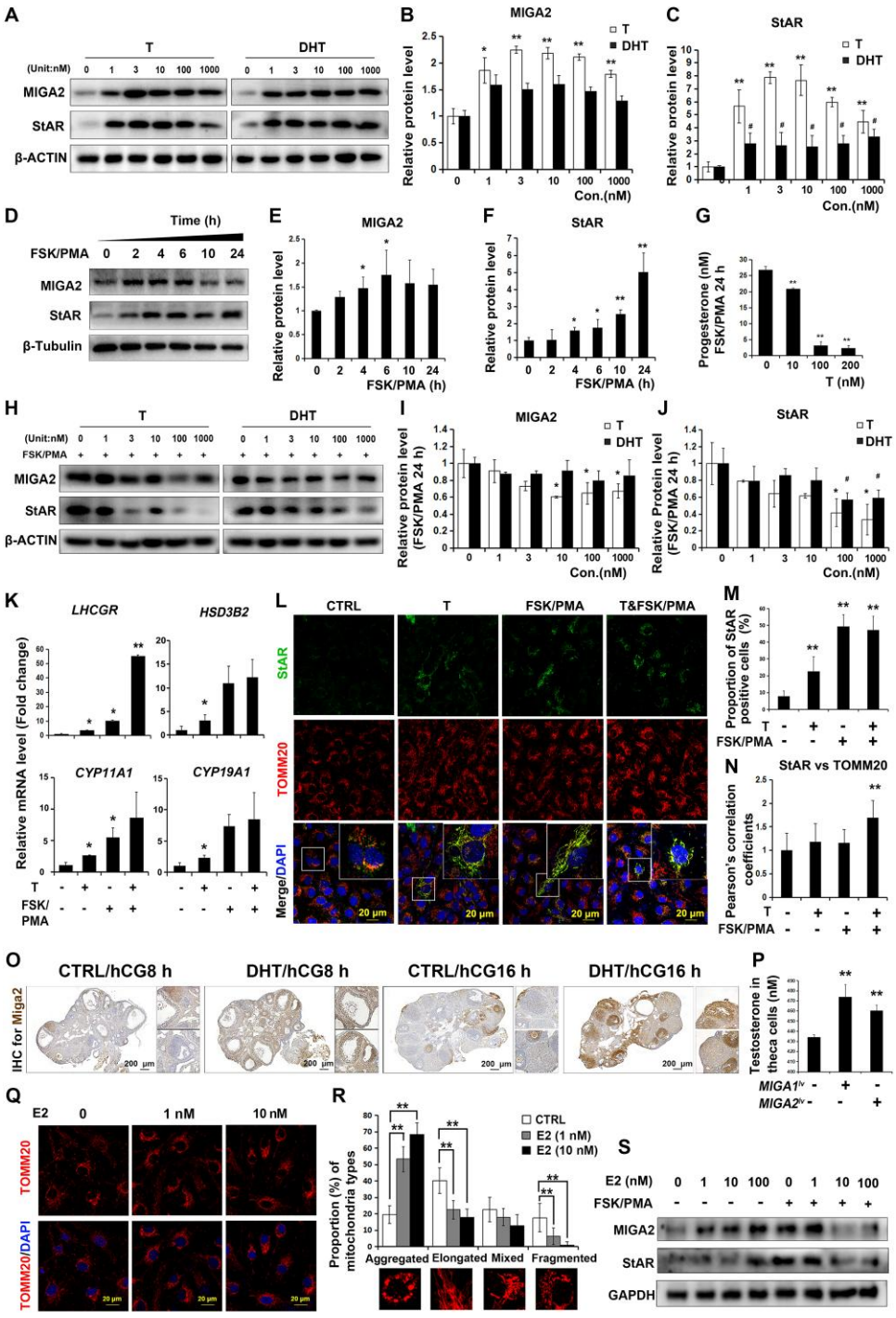

Figure 4. MIGA2 and StAR expression is regulated by T/DHT in ovarian granulosa cells. (A) T or DHT treatments at the indicated concentrations for 24 hours increased MIGA2 and StAR protein expression levels in KGN cells. (B, C) Quantification of MIGA2 (B) and StAR (C) protein expression for data in (A). (D) FSK/PMA treatments for different times increased MIGA2 and StAR protein expression in a time-dependent manner. (E, F) Quantification of protein expression of MIGA2 (E) and StAR (F) for data in (D). (G) Progesterone levels were significantly decreased by the testosterone (10-200 nM) after the treatment of FSK/PMA for 24 hours. (H-J) T or DHT at the indicated concentrations (1-1000 nM) decreased the protein expression of MIGA2 (I) and StAR (J) after combined treatment of FSK/PMA for 24 hours. (K) The mRNA expression of *LHCGR*, *CYP11A,1*, *CYP19A1*, and *HSD3B2* after the treatments of T (100 nM) or FSK/PMA as indicated. (L) Immunofluorescence images showed StAR and TOMM20 expression with the same treatments as in (K). (M) Proportions of StAR-positive cells in (L). (N) Pearson's correlation coefficients of StAR and TOMM20. (O) Immunohistochemistry for Miga2 protein expression in mouse ovaries injected with DHT followed with PMSG 48 hours and hCG 8 hours or hCG 16 hours. (P) T levels after MIGA1 and MIGA2 overexpression in mouse theca cells. (Q) Immunofluorescence of KGN cells after the treatment of different concentrations (1-100 nM) of E2 for 24 hours. (R) Proportion of cells with different mitochondrial morphology types after E2 treatment for 24 hours. (S) Representative western blot images of MIGA2 and StAR after treatments of different concentrations (1-100 nM) of E2 with or without FSK/PMA. Statistical significance of difference was compared to the control. Data presented as mean ± SD. *, $P < .05$, **, $P < .01$.

Abbreviations: DHT, dihydrotestosterone; E2, estradiol; hCG, human chorionic gonadotropin; MIGA1, mitoguardin 1; MIGA2, mitoguardin 2; PMSG, pregnant mare serum gonadotropin; StAR, steroidogenic acute regulatory protein; T, testosterone; TOMM20, translocase of outer mitochondrial membrane 20.

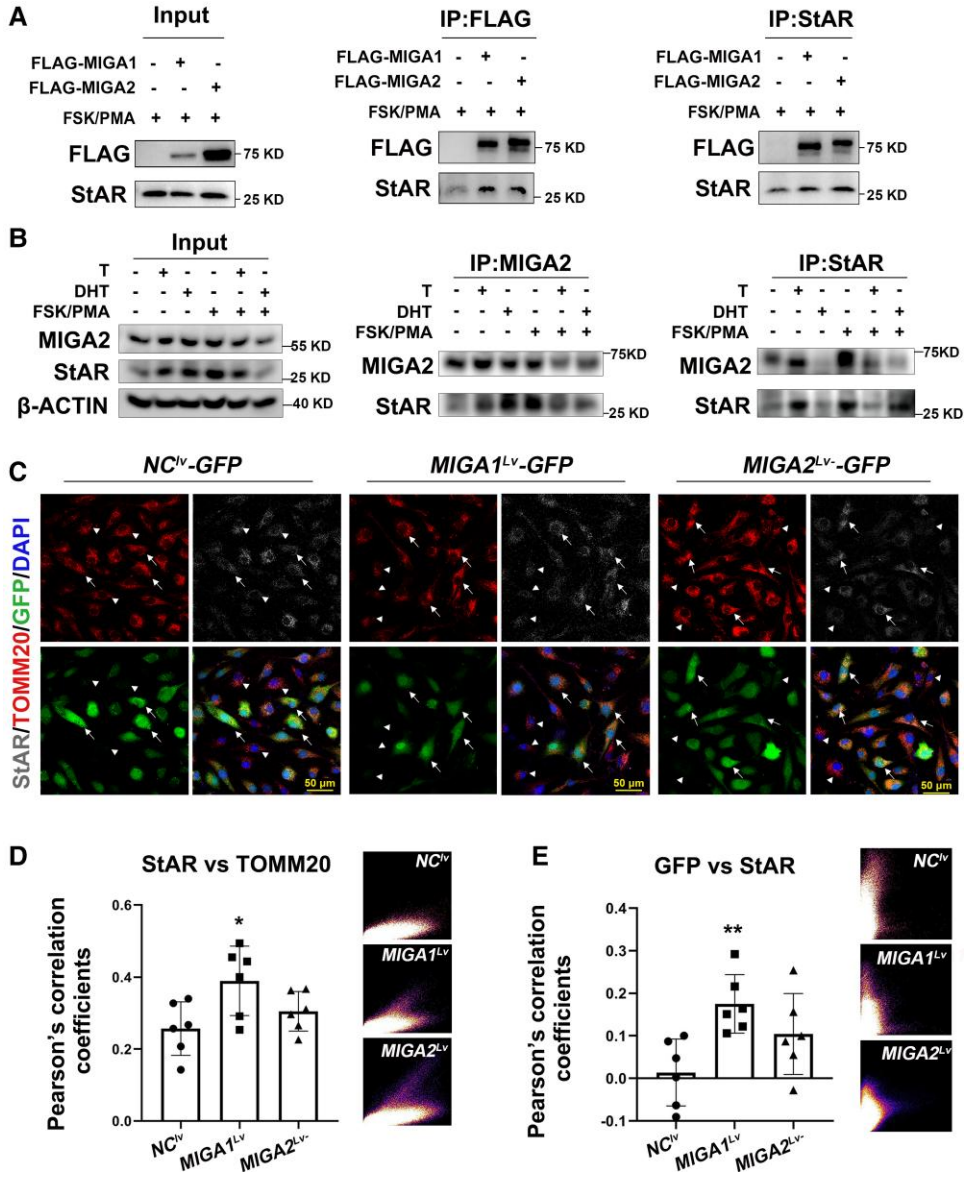

Figure 5. MIGA1 and MIGA2 interact with StAR and induce StAR localization on mitochondria. (A) IP experiments in KGN cells showed that FLAG tagged MIGA1 or MIGA2 could pull down StAR, and StAR could pull down the FLAG tagged MIGA1 and MIGA2. (B) IP experiments detected endogenous interaction between MIGA2 and StAR after T or DHT treatment with FSK/PMA 24 hours or not. (C) Immunofluorescence for TOMM20 and StAR after MIGA1-GFP or MIGA2-GFP overexpression and FSK/PMA treatment for 24 hours. Arrows indicated that the fluorescence signal of GFP was very strong, and arrowheads indicated that the fluorescence signal of GFP was very weak. (D, E) The Pearson's correlation coefficients and the scatterplots for TOMM20 and StAR (D), GFP, and StAR (E) after MIGA1-GFP or MIGA2-GFP overexpression in KGN cells. Statistical significance of difference was compared to the NC. Data presented as mean ± SD. *, $P < .05$, **, $P < .01$.
Abbreviations: DHT, dihydrotestosterone; FSK, forskolin; IP, immunoprecipitation; MIGA1, mitoguardin 1; MIGA2, mitoguardin 2; NC, negative control; PMA, phorbol 12-myristate 13-acetate; StAR, steroidogenic acute regulatory protein; T, testosterone; TOMM20, translocase of outer mitochondrial membrane 20.

antagonist flutamide (Sigma) to block androgen actions through AR. The results showed that AR expression was significantly increased after treatment with testosterone (1000 nM) compared with the control, and significant increases in AR levels were observed after combined treatment of flutamide with testosterone (50-100 nM) compared with the testosterone alone (Fig. 6A). This suggested that AR could be induced by high testosterone concentrations and induced by negative feedback regulation at concentrations of 50 to 100 nM. Treatment of flutamide (5 μM) combined with the indicated concentration of testosterone significantly increased the mRNA expression of *MIGA1* and *MIGA2*, compared with the testosterone treatment alone (Fig. 6B and 6C), suggesting that testosterone might promote MIGA1, −2 expressions through other pathways besides AR.

In addition, it was found testosterone (10 nM, 100 nM) treatment significantly increased LHCGR protein levels, and flutamide combined with testosterone (0-10 nM) treatment still significantly increased LHCGR protein expression compared with testosterone treatment alone (Fig. 6D and 6E). Furthermore, treatment of testosterone (10-100 nM) but not DHT significantly increased the LHCGR protein level (Fig. 6F and 6G); however, treatment of testosterone (≥3 nM) or DHT (≥1 nM) reduced the LHCGR protein expression after FSK/PMA treatment for 24 hours (Fig. 6H and 6I). These findings suggested that testosterone might

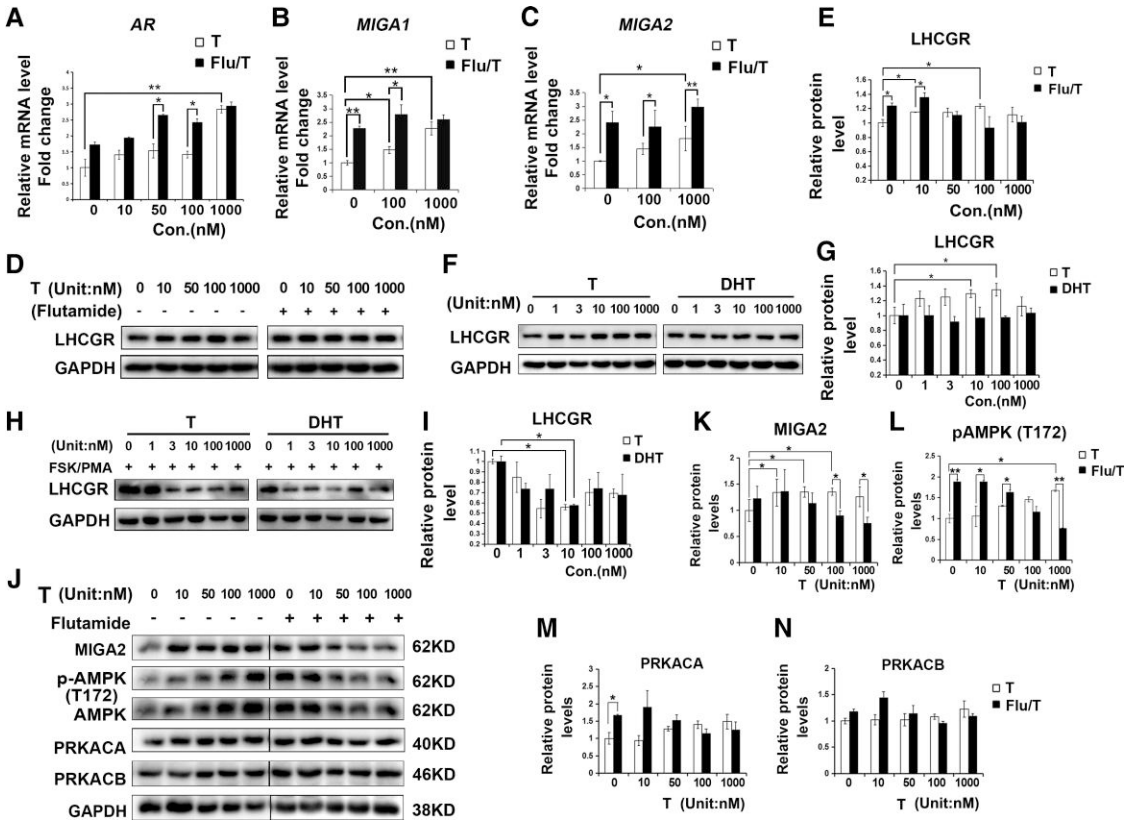

Figure 6. T-regulated MIGA2 expression dependent on androgen receptor in a concentration dependent manner in KGN cells. (A) Relative mRNA expression of AR after treatments of T at indicated concentrations or combined treatment of Flu (5 μM). (B, C) Relative mRNA expression of MIGA1 (B) and MIGA2 (C) after treatments of indicated concentrations of T or combined treatment of Flu. (D, E) LHCGR protein expression after the indicated concentrations of T or combined treatment of Flu. (F-I) LHCGR protein expression levels after the indicated treatment of gradient concentration of T or DHT (F, G), or treatments of T or DHT combined with FSK/PMA for 24 hours (H, I). (J-N) Representative western blots of MIGA2, pAMPK (T172), AMPK, PRKACA, and PRKACB after treatments of T at indicated concentrations or combined treatment of Flu (5 μM) (L). Quantification of relative protein expression levels of MIGA2 (J) pAMPK (K), PRKACA (M), and PRKACB (N). Data presented as mean ± SD. *, $P < .05$, **, $P < .01$.
Abbreviations: AMPK, AMP-activated protein kinase; AR, androgen receptor; DHT, dihydrotestosterone; Flu, flutamide; FSK, forskolin; LHCGR, LH/choriogonadotropin receptor; MIGA1, mitoguardin 1; MIGA2, mitoguardin 2; pAMPK, phosphorylation of AMPK; PMA, phorbol 12-myristate 13-acetate; PRKACA, PKA catalytic subunit α; PRKACB, PKA catalytic subunit β; T, testosterone.

promote MIGA1 and MIGA2 expression partially through LHCGR besides AR.

To detect the involved signaling pathways of testosterone regulation on MIGA2, PKA and AMPK signals were detected. Different concentrations of testosterone treatments were found to increase the expression of MIGA2 and pAMPK at T172 in a concentration-dependent manner. Flutamide (5 μM) treatment alone could increase MIGA2 and pAMPK (T172) protein levels, while when added with flutamide at high testosterone levels (100-1000 nM), MIGA2 and pAMPK (T172) protein levels were suppressed compared with testosterone treatment alone (Fig. 6J-L). In addition, the PKA subunits PRKACA and PRKACB showed an increased tendency with different concentrations of testosterone treatment, and flutamide treatments increased PRKACA expression compared with the control but showed no obvious effect on PRKACB expression (Fig. 6J, 6M, 6N).

Testosterone Might Regulate MIGA1, 2 and StAR Through PKA/AMPK Pathway

To detect whether MIGA1 and MIGA2 regulate PKA or AMPK signaling, we detected PKA or AMPK levels after MIGA1 and MIGA2 overexpression. It was found MIGA1 and MIGA2 overexpression significantly increased PRKACA expression. While PRKACA expression was inhibited significantly by FSK/PMA treatment for 24 hours, meanwhile, PRKACB expression was induced by FSK/PMA treatment and MIGA2 overexpression significantly induced PRKACB expression (Fig. 7A and 7B). To assess the effects on mitochondrial oxidative phosphorylation, MIGA1 or MIGA2 overexpression was found to increase the subunit of mitochondrial ATP synthase ATP5A levels after FSK/PMA treatment for 24 hours compared to the control (Fig. 7A and 7B). In addition, pAMPK (T172) levels were increased after MIGA1 and MIGA2 overexpression but decreased after FSK/PMA treatment for 24 hours even with MIGA1 overexpression, whereas there was no difference between FSK/PMA treated and untreated cells after MIGA2 overexpression (Fig. 7A and 7C). Furthermore, ATP levels were detected to be increased after MIGA1 and MIGA2 overexpression and decreased after FSK/PMA treatment for 24 hours, while it was increased significantly after MIGA2 overexpression upon FSK/PMA treatment for 24 hours (Fig. 7A and 7D).

The PKA inhibitor H-89 was applied to assess whether FSK/PMA regulated MIGA2 and StAR expression via PKA. As previously discovered, FSK/PMA treatment induced MIGA2 and StAR expression. H-89 (20 μM) treatment for 24 hours

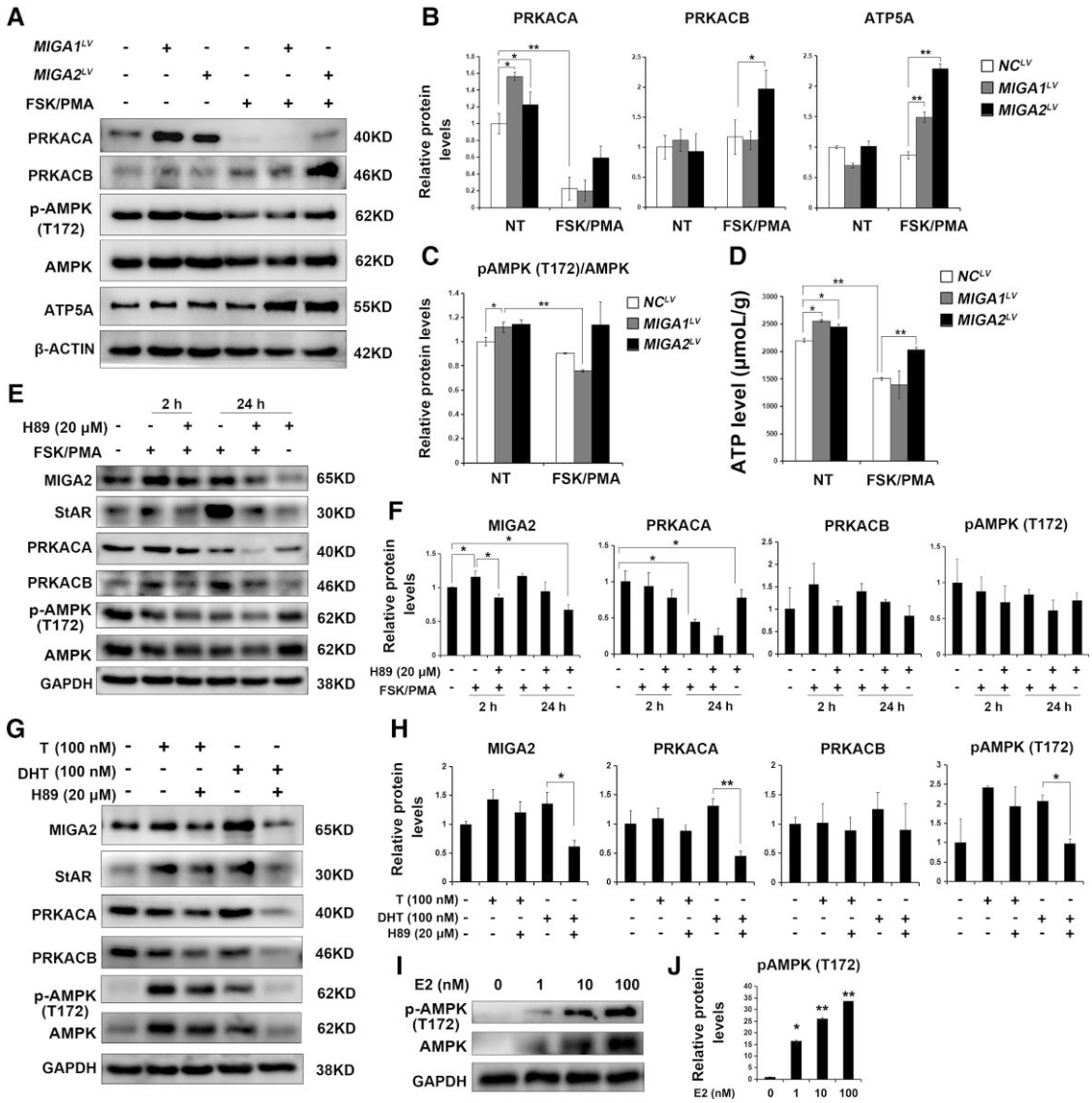

Figure 7. PKA and AMPK signalings are involved in testosterone regulation on MIGA2 and StAR. (A) Representative western blots of PRKACA, PRKACB, pAMPK (T172), AMPK, and ATP5A after MIGA1 or MIGA2 overexpression and treatments with FSK/PMA for 24 hours or not. (B) Quantification of the relative protein expression levels of PRKACA, PRKACB, and ATP5A to β-ACTIN in (B) compared to the control. (C) Quantification of phosphorylation of pAMPK (T172)/AMPK of (C). (D) ATP levels after MIGA1 or MIGA2 overexpression and treatments with FSK/PMA for 24 hours or not. (E) Representative western blots of MIGA2, StAR, PRKACA, PRKACB, pAMPK (T172), and AMPK after FSK/PMA or H-89 treatments for 2 or 24 hours. (F) Quantification of the relative protein expression levels of (E) to GAPDH compared to the control. (G) Representative western blots of MIGA2, StAR, PRKACA, PRKACB, pAMPK (T172), and AMPK after T, DHT, or H-89 treatments for 24 hours. (H) Quantification of relative protein expression levels of (G) to GAPDH compared to the control. (I, J) Representative western blots images of pAMPK (T172) and AMPK after E2 treatment for 24 hours at the concentration of 1, 10, 100 nM. (J) The quantification of relative protein expression levels of pAMPK (T172) to GAPDH compared to the control. Data presented as mean ± SD. *, $P < .05$, **, $P < .01$.

Abbreviations: AMPK, AMP-activated protein kinase; DHT, dihydrotestosterone; E2, estradiol; FSK, forskolin; MIGA1, mitoguardin 1; MIGA2, mitoguardin 2; pAMPK, phosphorylation of AMPK; PKA, cAMP-activated protein kinase A; PMA, phorbol 12-myristate 13-acetate; PRKACA, PKA catalytic subunit α; PRKACB, PKA catalytic subunit β; StAR, steroidogenic acute regulatory protein; T, testosterone.

inhibited MIGA2 expression, and the action of FSK/PMA on MIGA2 and StAR was abrogated by H-89 (Fig. 7E and 7F). The PKA subunits PRKACA was significantly inhibited after FSK/PMA treatment for 24 hours but not at 2 hours, and the expression was further inhibited by the pretreatment of H-89. In contrast, PRKACB was increased by FSK/PMA treatment, and the increases could be abrogated by H-89. In addition, FSK/PMA treatment decreased pAMPK (T172) levels, while H-89 addition showed no obvious changes in pAMPK (T172) or AMPK levels (Fig. 7E and 7F). To further detect whether testosterone regulated MIGA2 expression partially through LHCGR-mediated functions, H-89 was applied in combination with testosterone or DHT. Results showed that the increases in MIGA2 and StAR expression induced by testosterone or DHT were abrogated by H-89. Also, PRKACA and PRKACB expression was suppressed by the combined treatment of DHT and H-89 compared with DHT treatment alone. The increased levels of pAMPK (T172) induced by testosterone or DHT could also be abrogated by H-89, especially in cells treated with DHT (Fig. 7G and 7H). The results indicated that testosterone might exhibit an additional function of E2 on AMPK activation. To further identify the action of E2,

we assessed the protein expression of pAMPK (T172) and AMPK after E2 treatments at indicated concentrations. The results showed that E2 increased pAMPK (T172) and AMPK expression in a concentration-dependent manner (Fig. 7I and 7J), which further explained the stronger functions of testosterone than that of DHT.

Discussion

Recent studies suggested that testosterone increased mitochondrial activities and promoted the proliferation of granulosa cells in mouse antral follicles [41]. Testosterone and estrogen, especially estrogen, regulated mitochondrial dynamics through MFN1, MFN2, OPA1, and DRP1 in cardiovascular disease, which is an increased risk in women with PCOS [42]. However, little is known about the effect of testosterone on mitochondrial dynamics in ovarian granulosa cells of PCOS women. This study confirmed the correlation between serum testosterone and mitochondrial fusion mediated by MIGA1, −2 in granulosa cells and revealed that exogenous testosterone could disrupt steroidogenesis by regulating MIGA2 and PKA/AMPK signaling in human granulosa cells.

In this study, PCOS women with hyperandrogenism had high serum testosterone and E2 levels. The expression of MIGA1 and MIGA2 both positively correlated with serum testosterone levels. Further study indicated testosterone induced mitochondrial aggregation or elongation and significantly increased MIGA2 expression, while DHT showed relatively weak effects. This is because testosterone could be converted to both DHT and E2, and E2 has been proven to promote mitochondrial aggregation and MIGA2 protein expression in granulosa cells. However, DHT has no such effects since it could not be aromatized and only act through the AR. Nevertheless, DHT was found to increase Miga2 expression in mouse ovulating granulosa cells. This was consistent with the results of elevated *MIGA1, −2* expression in granulosa cells of PCOS women with hyperandrogenism, further confirming the association between hyperandrogenism and MIGA2 expression in granulosa cells. However, the expression of other mitochondrial dynamics-related genes such as MFN1, MFN2, OPA1, and DRP1 in hyperandrogenogenic granulosa cells remains unclear, and whether E2 regulates these mitochondrial dynamic-related genes in granulosa cells remains to be confirmed.

Recent studies indicated that testosterone could still induce PCOS-like features of irregular cycles and anovulation in AR-knockout mice but DHT did not [43]. This suggested that indirect actions of androgens were still able to induce PCOS features through pathways other than AR. In the present study, we found that testosterone could regulate MIGA1/2 expression independent of AR; however, LHCGR was synchronously regulated with MIGA2 on protein levels. Studies indicated that the polymorphism of LHCGR gene was associated with testosterone levels in males [44]. It is hypothesized that testosterone may induce MIGA2 expression in part through LHCGR-mediated signaling other than AR. However, the regulatory mechanism of testosterone on LHCGR remains unclear.

Studies indicated that MFN2 knockdown reduced StAR localization on mitochondria and inhibited progesterone biosynthesis after hCG or cAMP stimulation in Leydig cells [45]. LH increased DRP1 Ser 637 phosphorylation and resulted in mitochondrial elongation, and the knockdown of DRP1 increased basal and LH-induced progesterone levels via PKA signaling in bovine luteal cells [46]. Our previous studies indicated that knocking out *Miga1, −2* genes in female mice led to decreased progesterone levels in granulosa cells, ovulation disorder, and oocyte meiosis deficiency [34, 47], which were similar to functions of MFN1, −2 in the ovary. In the present study, it was found MIGA2 expression was increased by FSK/PMA from 2 hours to 6 hours but descended from10 hours to 24 hours. In addition, Miga2 was highly expressed in DHT-induced mouse granulosa cells of ovulating follicles but decreased in corpus luteal compared with that in ovulating follicles. These results suggested that MIGA2 expression was regulated by hCG or FSK/PMA in a time-dependent manner, and MIGA2 might play a more important role in ovulation than in luteal formation. StAR expression was also induced by FSK/PMA in a time-dependent manner. MIGA2 interacted with StAR and induced StAR localization on mitochondria, but MIGA2 overexpression inhibited StAR protein expression. As a result, MIGA2 overexpression significantly reduced progesterone levels in luteal cells. This seemed to contradict the results of *Miga2* knockout or DRP1 knockdown, which might be due to different regulatory mechanisms or gain of function upon MIGA2 overexpression. Testosterone or DHT also increased StAR expression in a similar way as MIGA2. However, MIGA2 and StAR protein expression was diminished after combined treatments of testosterone or DHT with FSK/PMA. It is speculated that excess androgens may increase mitochondrial fusion through MIGA2, which increases the expression of LH-targeted genes of *CYP11A1* and *HSD3B2* in granulosa cells, thereby inducing early luteinization of granulosa cells and preventing small follicles from maturing and ovulating; however, the androgens would inhibit progesterone synthesis by reducing mitochondrial fusion levels and StAR expression when LH surges. Clinically, polymorphism of the *CYP11A* gene had been found to be strongly associated with PCOS and hyperandrogenism [48]. CYP19A1 (aromatase) that localized to the ER was suggested to be included as a genetic modifier of PCOS [49]. HSD3B2 was found localized on the lipid droplet, except for the ER and mitochondria, to convert the pregnenolone to progesterone in adrenal lipids. CYP11A1 as well as HSD3B2 was also detected in lipid droplets in rat primary granulosa cells [50, 51]. In the present study, *MIGA2* overexpression significantly increased *CYP11A1*, *CYP19A1,* and *HSD3B2* expression in luteal cells. Interestingly and worthy of further analysis, testosterone might promote lipogenesis through MIGA2 by communicating the subcellular organelles, such as mitochondria, ER, and the lipid droplets, and play a key role in lipogenesis in adipocytes by regulating these steroidogenic-related genes [31, 52].

This study further found that MIGA1/2 overexpression increased the protein levels of PKA subunit PRKACA, which were both inhibited by FSK/PMA. In contrast, PRKACB was induced by FSK/PMA, and MIGA2 overexpression could significantly increase PRKACB levels upon FSK/PMA treatment. This suggested that PRKACA might primarily act in granulosa cells during follicle growth, whereas PRKACB might act primarily in luteinization during LH surge. In addition, MIGA2 expression was significantly induced by FSK/PMA at 2 hours but slightly diminished at 24 hours when PRKACA expression was significantly inhibited and PRKACB was induced, suggesting a possible role of PKA on MIGA2 expression. Inhibition of PKA significantly inhibited basic and FSK/PMA-induced MIGA2 expression.

This suggested that FSK/PMA induced MIGA2 expression via PKA and PRKACA reduction might further reduce MIGA2 expression, whereas PRKACB increase could only maintain a relatively lower MIGA2 level compared to PRKACA. In addition, MIGA2 overexpression increased pAMPK (T172) but reduced StAR expression and progesterone levels in luteal cells. However, whether activation of AMPK inhibited StAR and decreased progesterone in human granulosa cells remained unknown. Recent studies had shown that AMPK activation inhibited LH-stimulated progesterone production without reducing StAR protein but increased hormone-sensitive lipase phosphorylation at Ser 565 and inhibited HSL phosphorylation at Ser 563, thereby inhibiting hormone-sensitive lipase activation and preventing hydrolysis of cholesteryl esters in lipid droplets, and exogenous cholesterol reversed the inhibitory effect of AMPK on progesterone production. It suggested that AMPK inhibited progesterone production by limiting cholesterol availability. In addition, pAMPK (T172) was reduced by LH/PKA and could be rescued by the PKA inhibitor in bovine luteal cells [28]. In this study, pAMPK (T172) was also found to decrease after FSK/PMA treatments, which might be inhibited by PRKACB or due to the loss of PRKACA, which was consistent with the aforementioned findings. However, H-89 (20 μM) treatments for 2 or 24 hours were unable to rescue pAMPK (T172) levels, which might be due to the relatively low concentration or the long treatment times. Studies indicated that testosterone could promote glucose metabolism through AMPK in cardiomyocytes [53]. This study also found that testosterone or DHT increased pAMPK (T172) levels in granulosa cells. The PKA inhibitor H-89 reduced testosterone- or DHT-induced pAMPK (T172) levels and significantly inhibit DHT-induced pAMPK (T172) in particular. This indicated that testosterone/DHT induced pAMPK (T172) via PKA. It was suggested that DHT actioned through AR and promoted MIGA2 expression, then MIGA2 overexpression increased pAMPK (T172) through PRKACA. It was speculated that testosterone might increase pAMPK (T172) partially through LHCGR. In addition, AR-mediated PKA, which inhibited pAMPK (T172) levels in granulosa cells, thereby H-89 showed a relative weak effect on the inhibition of testosterone-induced pAMPK (T172).

There are still some limitations and unanswered questions in this study. Further mechanistic studies in primary human granulosa cells are difficult due to the unavailability and short survival time of granulosa cells from individual patients. Thus, in this study, KGN cells were used for the overexpression of genes of interest and for drug treatments. However, more evidence should be provided, including the evidence for MIGA2 and StAR protein interactions, and in vivo validations of the regulatory role of testosterone in LHCGR and PKA/AMPK signaling pathways. Whether MIGA2 regulates glucose metabolism through AMPK in granulosa cells remains to be studied.

In summary, expression of MIGA1 and MIGA2 in granulosa cells is associated with hyperandrogenism in PCOS patients, and excess testosterone increases MIGA2 expression via AR or possibly LHCGR in part. Increases of cAMP induced by FSK/PMA regulate MIGA2 expression through PKA in a time-dependent manner. Both testosterone and FSK/PMA enhance the interaction of MIGA2 with StAR on mitochondria. However, MIGA2 overexpression inhibits StAR expression and regulates steroidogenesis by reducing progesterone levels and increasing the aromatization of testosterone to E2 (Fig. 8). This study uncovers opposing functions between testosterone effects and cAMP effects on AMPK activity via PKA signaling in granulosa cells. This study provides new clues about testosterone functions on mitochondrial activity and functions in granulosa cells. Disordered mitochondrial fusion is suggested as a novel mechanism of ovulatory dysfunction in PCOS patients with hyperandrogenism. This study may also provide clues for the development of mitochondria-targeted drugs for metabolic diseases such as

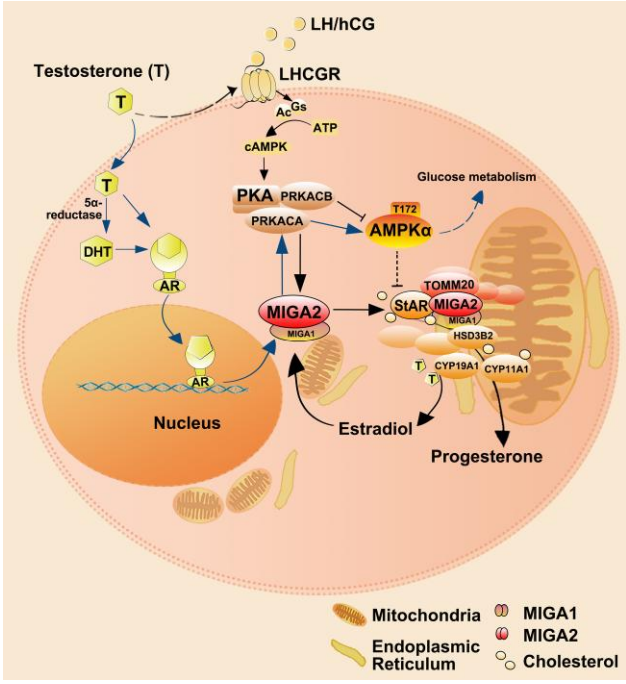

Figure 8. Proposed schematic representation of testosterone regulation through MIGA2 during steroidogenesis in ovarian granulosa cells. Testosterone may promote mitochondrial fusion mediated by MIGA1/2 via AR or LHCGR partially. LH or hCG binds to LHCGR and activates PKA through Gs-mediated activation of Ac and the increase of cAMP. Likewise, FSK activates PKA and PMA activates PKC. Increase of cAMP regulates MIGA2 expression through PKA signaling in a time-dependent manner. MIGA2 increases TOMM20, interacts with StAR, and induces StAR localization on mitochondria in luteal cells. Testosterone or FSK/PMA increases the expression and interactions of MIGA2 and StAR. However, MIGA2 overexpression increases PRKACA and pAMPK (T172) levels but inhibits StAR protein expression. The pAMPK (T172) is speculated to be increased by PRKACA subunit but inhibited by PRKACB subunit and has been suggested to play a role in inhibiting progesterone synthesis. The key steroidogenic genes of *CYP11A1, HSD3B2,* and *CYP11A1* were all increased by either testosterone or MIGA2 overexpression. As a result, MIGA2 decreases progesterone levels but increases estradiol levels by promoting the aromatization of testosterone. In addition, estradiol regulates MIGA2 expression in turn. However, whether MIGA2 regulates steroidogenesis via AMPK in granulosa cells remains to be clarified. Ac, Abbreviations: Ac, adenylyl cyclase; AR, androgen receptor; BMI, body mass index; FSK, forskolin; Gs, stimulatory G proteins that activate Ac; HA-PCOS, 75 hyperandrogenic PCOS; hCG, human chorionic gonadotropin; LHCGR, LH/choriogonadotropin receptor; MIGA1, mitoguardin 1; MIGA2, mitoguardin 2; NA-PCOS, 54 normo-androgenic PCOS; PCOS, polycystic ovary syndrome; PKA, cAMP-activated protein kinase A; PMA, phorbol 12-myristate 13-acetate; PKC, protein kinase C; StAR, steroidogenic acute regulatory protein; TOMM20, translocase of outer mitochondrial membrane 20.

hyperandrogenemia or obesity by targeting the molecular structure of MIGA2.

Acknowledgments

The authors thank all participants in this study. The authors would like to thank Hongbin Liu and Shigang Zhao for their help on clinical data analysis.

Funding

This study was funded by National Natural Science Foundation of China (81601241), Natural Science Foundation of Shandong Province (ZR2021MH056, ZR2016HB31), and Clinical Medical Science and Technology Innovation Program of Jinan City (201805068).

Disclosures

The authors have nothing to disclose.

Data Availability

Original data generated and analyzed during this study are included in this published article or in the data repositories listed in References.

References

1. Bozdag G, Mumusoglu S, Zengin D, Karabulut E, Yildiz BO. The prevalence and phenotypic features of polycystic ovary syndrome: a systematic review and meta-analysis. *Hum Reprod*. 2016;31-(12):2841-2855. doi:10.1093/humrep/dew218
2. Dumesic DA, Oberfield SE, Stener-Victorin E, Marshall JC, Laven JS, Legro RS. Scientific statement on the diagnostic criteria, epidemiology, pathophysiology, and molecular genetics of polycystic ovary syndrome. *Endocr Rev*. 2015;36(5):487-525. doi:10.1210/er.2015-1018
3. Dumesic DA, Richards JS. Ontogeny of the ovary in polycystic ovary syndrome. *Fertil Steril*. 2013;100(1):23-38. doi:10.1016/j.fertnstert.2013.02.011
4. Azziz R, Carmina E, Dewailly D, *et al*. Positions Statement: criteria for defining polycystic ovary syndrome as a predominantly hyperandrogenic syndrome: an androgen excess society guideline. *J Clin Endocrinol Metab*. 2006;91(11):4237-4245. doi:10.1210/jc.2006-0178
5. Rosenfield RL, Ehrmann DA. The pathogenesis of polycystic ovary syndrome (PCOS): the hypothesis of PCOS as functional ovarian hyperandrogenism revisited. *Endocr Rev*. 2016;37(5):467-520. doi:10.1210/er.2015-1104
6. O'Reilly MW, Kempegowda P, Jenkinson C, *et al*. 11-Oxygenated C19 steroids are the predominant androgens in polycystic ovary syndrome. *J Clin Endocrinol Metab*. 2017;102(3):840-848. doi:10.1210/jc.2016-3285
7. Skarra DV, Hernández-Carretero A, Rivera AJ, Anvar AR, Thackray VG. Hyperandrogenemia induced by letrozole treatment of pubertal female mice results in hyperinsulinemia prior to weight gain and insulin resistance. *Endocrinology*. 2017;158(9):2988-3003. doi:10.1210/en.2016-1898
8. Fazakerley DJ, Minard AY, Krycer JR, *et al*. Mitochondrial oxidative stress causes insulin resistance without disrupting oxidative phosphorylation. *J Biol Chem*. 2018;293(19):7315-7328. doi:10.1074/jbc.RA117.001254
9. Jheng H, Tsai P, Guo S, *et al*. Mitochondrial fission contributes to mitochondrial dysfunction and insulin resistance in skeletal muscle. *Mol Cell Biol*. 2012;32(2):309-319. doi:10.1128/MCB.05603-11
10. Zhang J, Bao Y, Zhou X, Zheng L. Polycystic ovary syndrome and mitochondrial dysfunction. *Reprod Biol Endocrinol*. 2019;17(1):67. doi:10.1186/s12958-019-0509-4
11. Sulaiman MA, Al-Farsi YM, Al-Khaduri MM, Saleh J, Waly MI. Polycystic ovarian syndrome is linked to increased oxidative stress in Omani women. *Int J Womens Health*. 2018;10:763-771. doi:10.2147/IJWH.S166461
12. Saeed N, Hamzah IH, Al-Gharrawi SAR. Polycystic ovary syndrome dependency on mtDNA mutation; copy number and its association with insulin resistance. *BMC Res Notes*. 2019;12(1):455. doi:10.1186/s13104-019-4453-3
13. Ye M, Hu B, Shi W, Guo F, Xu C, Li S. Mitochondrial DNA 4977 bp deletion in peripheral blood is associated with polycystic ovary syndrome. *Front Endocrinol (Lausanne)*. 2021;12:675581. doi:10.3389/fendo.2021.675581
14. Lieber T, Jeedigunta SP, Palozzi JM, Lehmann R, Hurd TR. Mitochondrial fragmentation drives selective removal of deleterious mtDNA in the germline. *Nature*. 2019;570(7761):380-384. doi:10.1038/s41586-019-1213-4
15. Tur J, Pereira-Lopes S, Vico T, *et al*. Mitofusin 2 in macrophages links mitochondrial ROS production, cytokine release, phagocytosis, autophagy, and bactericidal activity. *Cell Rep*. 2020;32(8):108079. doi:10.1016/j.celrep.2020.108079
16. Salehi R, Mazier HL, Nivet AL, *et al*. Ovarian mitochondrial dynamics and cell fate regulation in an androgen-induced rat model of polycystic ovarian syndrome. *Sci Rep*. 2020;10(1):1021. doi:10.1038/s41598-020-57672-w
17. Owens LA, Kristensen SG, Lerner A, *et al*. Gene expression in granulosa cells from small antral follicles from women with or without polycystic ovaries. *J Clin Endocrinol Metab*. 2019;104(12):6182-6192. doi:10.1210/jc.2019-00780
18. Rone MB, Midzak AS, Issop L, *et al*. Identification of a dynamic mitochondrial protein complex driving cholesterol import, trafficking, and metabolism to steroid hormones. *Mol Endocrinol*. 2012;26(11):1868-1882. doi:10.1210/me.2012-1159
19. Yue X, Qian Y, Gim B, Lee I. Acyl-CoA-binding domain-containing 3 (ACBD3; PAP7; GCP60): a multi-functional membrane domain organizer. *Int J Mol Sci*. 2019;20(8):2028. doi:10.3390/ijms20082028
20. Saitoh T, Igura M, Obita T, *et al*. Tom20 recognizes mitochondrial presequences through dynamic equilibrium among multiple bound states. *EMBO J*. 2007;26(22):4777-4787. doi:10.1038/sj.emboj.7601888
21. Arakane F, King SR, Du Y, *et al*. Phosphorylation of steroidogenic acute regulatory protein (StAR) modulates its steroidogenic activity. *J Biol Chem*. 1997;272(51):32656-32662. doi:10.1074/jbc.272.51.32656
22. Labrie F, Simard J, Luu-The V, *et al*. Structure and tissue-specific expression of 3 beta-hydroxysteroid dehydrogenase/5-ene-4-ene isomerase genes in human and rat classical and peripheral steroidogenic tissues. *J Steroid Biochem Mol Biol*. 1992;41(3-8):421-435. doi:10.1016/0960-0760(92)90368-s
23. Miller WL, Auchus RJ. The molecular biology, biochemistry, and physiology of human steroidogenesis and its disorders. *Endocr Rev*. 2011;32(1):81-151. doi:10.1210/er.2010-0013
24. Papadopoulos V, Miller WL. Role of mitochondria in steroidogenesis. *Best Pract Res Clin Endocrinol Metab*. 2012;26(6):771-790. doi:10.1016/j.beem.2012.05.002
25. Zhang Q, Ren J, Wang F, *et al*. Mitochondrial and glucose metabolic dysfunctions in granulosa cells induce impaired oocytes of polycystic ovary syndrome through Sirtuin 3. *Free Radic Biol Med*. 2022;187:1-16. doi:10.1016/j.freeradbiomed.2022.05.010
26. Troncoso MF, Pavez M, Wilson C, *et al*. Testosterone activates glucose metabolism through AMPK and androgen signaling in cardiomyocyte hypertrophy. *Biol Res*. 2021;54(1):3. doi:10.1186/s40659-021-00328-4
27. Herzig S, Shaw RJ. AMPK: guardian of metabolism and mitochondrial homeostasis. *Nat Rev Mol Cell Biol*. 2018;19(2):121-135. doi:10.1038/nrm.2017.95

28. Przygrodzka E, Hou X, Zhang P, Plewes MR, Franco R, Davis JS. PKA And AMPK signaling pathways differentially regulate luteal steroidogenesis. *Endocrinology*. 2021;162(4):bqab015. doi:10.1210/endocr/bqab015
29. Taylor SS, Wallbott M, Machal EMF, *et al*. PKA Cβ: a forgotten catalytic subunit of cAMP-dependent protein kinase opens new windows for PKA signaling and disease pathologies. *Biochem J*. 2021;478(11):2101-2119. doi:10.1042/BCJ20200867
30. Zhang YP, Liu XM, Bai J, *et al*. Mitoguardin regulates mitochondrial fusion through MitoPLD and is required for neuronal homeostasis. *Mol Cell*. 2016;61(1):111-124. doi:10.1016/j.molcel.2015.11.017
31. Freyre CAC, Rauher PC, Ejsing CS, Klemm RW. MIGA2 links mitochondria, the ER, and lipid droplets and promotes de novo lipogenesis in adipocytes. *Mol Cell*. 2019;76(5):811-825.e14. doi:10.1016/j.molcel.2019.09.011
32. Xu L, Wang X, Zhou J, *et al*. Miga-mediated endoplasmic reticulum-mitochondria contact sites regulate neuronal homeostasis. *Elife*. 2020;9:e56584. doi:10.7554/eLife.56584
33. Kim H, Lee S, Jun Y, Lee C. Structural basis for mitoguardin-2 mediated lipid transport at ER-mitochondrial membrane contact sites. *Nat Commun*. 2022;13(1):3702. doi:10.1038/s41467-022-31462-6
34. Liu XM, Zhang YL, Ji SY, *et al*. Mitochondrial function regulated by mitoguardin-1/2 is crucial for ovarian endocrine functions and ovulation. *Endocrinology*. 2017;158(11):3988-3999. doi:10.1210/en.2017-00487
35. Nishi Y, Yanase T, Mu Y, *et al*. Establishment and characterization of a steroidogenic human granulosa-like tumor cell line, KGN, that expresses functional follicle-stimulating hormone receptor. *Endocrinology*. 2001;142(1):437-445. doi:10.1210/endo.142.1.7862
36. Rotterdam ESHRE/ASRM-Sponsored PCOS Consensus Workshop Group. Revised 2003 consensus on diagnostic criteria and long-term health risks related to polycystic ovary syndrome (PCOS). *Hum Reprod*. 2004;19(1):41-47. doi:10.1093/humrep/deh098
37. Ji SY, Liu XM, Li BT, *et al*. The polycystic ovary syndrome-associated gene Yap1 is regulated by gonadotropins and sex steroid hormones in hyperandrogenism-induced oligo-ovulation in mouse. *Mol Hum Reprod*. 2017;23(10):698-707. doi:10.1093/molehr/gax046
38. Fan HY, Shimada M, Liu Z, *et al*. Selective expression of KrasG12D in granulosa cells of the mouse ovary causes defects in follicle development and ovulation. *Development*. 2008;135(12):2127-2137. doi:10.1242/dev.020560
39. Pfaffl MW. A new mathematical model for relative quantification in real-time RT-PCR. *Nucleic Acids Res*. 2001;29(9):e45. doi:10.1093/nar/29.9.e45
40. Yan MQ, Wang Y, Wang Z, *et al*. Supplementary data for: Mitoguardin2 is associated with hyperandrogenism and regulates steroidogenesis in human ovarian granulosa cells. Harvard Dataverse 2023. Deposited February 3, 2023. https://doi.org/10.7910/DVN/QMVIDF
41. Hoque SAM, Kawai T, Zhu Z, Shimada M. Mitochondrial protein turnover is critical for granulosa cell proliferation and differentiation in antral follicles. *J Endocr Soc*. 2018;3(2):324-339. doi:10.1210/js.2018-00329
42. Lynch S, Boyett JE, Smith MR, Giordano-Mooga S. Sex hormone regulation of proteins modulating mitochondrial metabolism, dynamics and inter-organellar cross talk in cardiovascular disease. *Front Cell Dev Biol*. 2021;8:610516. doi:10.3389/fcell.2020.610516
43. Aflatounian A, Edwards MC, Rodriguez Paris V, *et al*. Androgen signaling pathways driving reproductive and metabolic phenotypes in a PCOS mouse model. *J Endocrinol*. 2020;245(3):381-395. doi:10.1530/JOE-19-0530
44. Liu W, Han B, Zhu W, *et al*. Polymorphism in the alternative donor site of the cryptic exon of LHCGR: functional consequences and associations with testosterone level. *Sci Rep*. 2017;7(1):45699. doi:10.1038/srep45699
45. Duarte A, Castillo AF, Podesta EJ, Poderoso C. Mitochondrial fusion and ERK activity regulate steroidogenic acute regulatory protein localization in mitochondria. *PLoS One*. 2014;9(6):e100387. doi:10.1371/journal.pone.0100387
46. Plewes MR, Hou X, Talbott HA, *et al*. Luteinizing hormone regulates the phosphorylation and localization of the mitochondrial effector dynamin-related protein-1 (DRP1) and steroidogenesis in the bovine corpus luteum. *FASEB J*. 2020;34(4):5299-5316.
47. Liu XM, Zhang YP, Ji SY, *et al*. Mitoguardin-1 and -2 promote maturation and the developmental potential of mouse oocytes by maintaining mitochondrial dynamics and functions. *Oncotarget*. 2016;7(2):1155-1167. doi:10.18632/oncotarget.6713
48. Gharani N, Waterworth DM, Batty S, *et al*. Association of the steroid synthesis gene CYP11a with polycystic ovary syndrome and hyperandrogenism. *Hum Mol Genet*. 1997;6(3):397-402. doi:10.1093/hmg/6.3.397
49. Xita N, Lazaros L, Georgiou I, Tsatsoulis A. CYP19 gene: a genetic modifier of polycystic ovary syndrome phenotype. *Fertil Steril*. 2010;94(1):250-254. doi:10.1016/j.fertnstert.2009.01.147
50. Yu J, Zhang L, Li Y, *et al*. The adrenal lipid droplet is a new site for steroid hormone metabolism. *Proteomics*. 2018;18(23):e1800136. doi:10.1002/pmic.201800136
51. Khor VK, Ahrends R, Lin Y, *et al*. The proteome of cholesteryl-ester-enriched versus triacylglycerol-enriched lipid droplets. *PLoS One*. 2014;9(8):e105047. doi:10.1371/journal.pone.0105047
52. Hong Z, Adlakha J, Wan N, *et al*. Mitoguardin-2-mediated lipid transfer preserves mitochondrial morphology and lipid droplet formation. *J Cell Biol*. 2022;221(12):e202207022. doi:10.1083/jcb.202207022
53. Mitsuhashi K, Senmaru T, Fukuda T, *et al*. Testosterone stimulates glucose uptake and GLUT4 translocation through LKB1/AMPK signaling in 3T3-L1 adipocytes. *Endocrine*. 2016;51(1):174-184. doi:10.1007/s12020-015-0666-y